Contract No:

This document was prepared in conjunction with work accomplished under Contract No. DE-AC09-08SR22470 with the U.S. Department of Energy (DOE) Office of Environmental Management (EM).

Disclaimer:

This work was prepared under an agreement with and funded by the U.S. Government. Neither the U. S. Government or its employees, nor any of its contractors, subcontractors or their employees, makes any express or implied:

1) warranty or assumes any legal liability for the accuracy, completeness, or for the use or results of such use of any information, product, or process disclosed; or
2) representation that such use or results of such use would not infringe privately owned rights; or
3) endorsement or recommendation of any specifically identified commercial product, process, or service.

Any views and opinions of authors expressed in this work do not necessarily state or reflect those of the United States Government, or its contractors, or subcontractors.

CRYO-ADSORBENT HYDROGEN STORAGE SYSTEMS FOR FUEL CELL VEHICLES

Dr. David Tamburello
Savannah River National Laboratory
Aiken, SC, USA

Dr. Bruce Hardy
Savannah River National Laboratory
Aiken, SC, USA

Dr. Claudio Corgnale
Savannah River Consulting
Aiken, SC, USA

Dr. Martin Sulic
Savannah River Consulting
Aiken, SC, USA

Dr. Donald Anton
Savannah River National Laboratory
Aiken, SC, USA

ABSTRACT

Numerical models for the evaluation of cryo-adsorbent based hydrogen storage systems for fuel cell vehicles were developed and validated against experimental data. These models simultaneously solve the equations for the adsorbent thermodynamics together with the conservation equations for heat, mass, and momentum. The models also use real gas thermodynamic properties for hydrogen. Model predictions were compared to data for charging and discharging both activated carbon and MOF-5™ systems. Applications of the model include detailed finite element analysis simulations and full vehicle-level system analyses. The full system models were used to compare prospective system design performance given specific options, such as the adsorbent materials, pressure vessel types, internal heat exchangers, and operating conditions. The full vehicle model, which also allows the user to compare adsorbent systems with compressed gas, metal hydride, and chemical hydrogen storage systems, is based on an 80 kW fuel cell with a 20 kW battery evaluated using standard drive cycles.

This work is part of the Hydrogen Storage Engineering Center of Excellence (HSECoE), which brings materials development and hydrogen storage technology efforts address onboard hydrogen storage in light duty vehicle applications. The HSECoE spans the design space of the vehicle requirements, balance of plant requirements, storage system components, and materials engineering. Theoretical, computational, and experimental efforts are combined to evaluate, design, analyze, and scale potential hydrogen storage systems and their supporting components against the Department of Energy (DOE) 2020 and Ultimate Technical Targets for Hydrogen Storage Systems for Light Duty Vehicles.

INTRODUCTION

Onboard hydrogen (H_2) storage is a major technical barrier to the development of practical H_2 fuel cell (FC) vehicles. With input from American automakers, the DOE has published a set of technical targets that must be met for H_2 vehicles to be competitive with modern gasoline/diesel vehicles [1]. While compressed, cryo-compressed, and liquefied hydrogen storage [2, 3] have shown great promise in FC vehicles, a significant amount of energy is required to put the H_2 in a liquefied or highly compressed state. For this reason, alternative approaches using media-based H_2 storage are being examined. The media-based storage can be separated into three general classifications: chemical hydrides [4, 5, 6] that are regenerated off-board; metal hydrides [7, 8, 9], which undergo chemical reactions during the charging process and are refueled onboard the vehicle; and adsorbents [10, 11, 12, 13, 14] that uptake H_2 via physisorption. The present work will focus on adsorbents.

The DOE formed the Hydrogen Storage Engineering Center of Excellence (HSECoE) to bring materials development and hydrogen storage technology efforts together to address onboard H_2 storage in light duty vehicle applications for all three media-based storage types. With respect to adsorbents, the HSECoE sought to create predictive adsorbent hydrogen storage computational models that have been validated experimentally by both excess adsorption measurements and laboratory-scale prototype adsorbent system evaluation. The hydrogen adsorption computational models have been used in detailed FEA studies to evaluate specific adsorbent-heat exchanger designs [14]. The adsorbent models have also been included in the HSECoE's full-scale vehicle framework model [15, 16] that is available for download from the HSECoE's webpage (www.hsecoe.org).

The present work uses these validated adsorbent computational models to perform a parametric analysis of possible onboard fuel cell vehicle adsorbent hydrogen storage systems. This parametric analysis was used to eliminate hydrogen storage technologies until only two adsorbent system designs remained, which were built into prototypes and tested at the conclusion of the HSECoE.

NOMENCLATURE

BOP	Balance of Plant
CcH2	Cryo-compressed Hydrogen
DOE	Department of Energy
EERE	Energy Efficiency and Renewable Energy
ENG	Expanded Natural Graphite
FCT	Fuel Cell Technologies
FEA	Finite Element Analysis
FTC	Flow-through cooling
H_2	Hydrogen gas
$H_{2,usable}$	Usable hydrogen gas (for vehicle FC operations)
HSECoE	Hydrogen Storage Engineering Center of Excellence
$-\Delta \overline{h_a^0}$	Isoteric heat of adsorption [J/mol]
L-to-D	Pressure vessel Length to diameter ratio
LN_2	Liquid Nitrogen
m	Distribution parameter, equal to 2 for most adsorbents
MATI	Modular Adsorbent Tank Insert
MLVI	Multi-layer vacuum insulation
n_a	Absolute adsorption per unit mass of adsorbent [mol/kg]
n_{ex}	Excess adsorption per unit mass of adsorbent [mol/kg]
n_{max}	Limiting adsorption per unit mass of adsorbent [mol/kg]
n_{tot}	Total amount of gas stored within the system volume [mol]
OSU	Oregon State University
P	Equilibrium pressure [Pa]
P_0	Pseudo-saturation pressure (within the adsorption model), [Pa]
PNNL	Pacific Northwest National Laboratory
PV	Pressure vessel
R	Universal gas constant [8.314 J/mol/K]
T	Equilibrium temperature [K]
V_a	Adsorption volume per unit mass of adsorption [m³/kg]
V_g	Interstitial volume within the adsorbent per unit mass of adsorbent [m³/kg]
V_v	Void volume of the adsorbent per unit mass of adsorption [m³/kg]
α	Enthalpic contribution to the characteristic free energy of adsorption [J/mol]
β	Entropic contribution to the characteristic free energy of adsorption [J/mol/K]
ε	Characteristic free energy of adsorption ($\varepsilon = \alpha + \beta T$), [J/mol]
ρ_g	Density of the bulk gas in equilibrium with the adsorbed phase [mol/m³]

ADSORBENT COMPUTATIONAL MODEL

The backbone of any adsorption-based computation is the adsorption theory used to describe the process. The Dubinin-Astakhov (D-A) model as described by Richard *et al* [10, 11] was chosen to describe the hydrogen adsorption isotherms needed to model the hydrogen storage within the vehicle model. The absolute adsorption (n_a) is given by the following equation:

$$n_a = n_{ex} + \rho_g V_a \qquad (1)$$

where n_{ex} is the excess adsorption, ρ_g is the bulk gas density, and V_a is the adsorption volume. The adsorption volume is interpreted as the volume of adsorption sites that can be micro-, meso-, and/or macropores within the adsorbent. The void space (void volume, V_v) within the adsorbent accounts for the pore space as well as the interstitial space within the adsorbent. The interstitial space within V_v where negligible adsorption takes place and where the density of the gas is the same as the bulk is defined as the gas volume:

$$V_g = V_v - V_a \qquad (2)$$

The void volume (V_v) is experimentally measured by helium probing or calculated from the bulk and skeletal density of the adsorbent.

Using the D-A model, the absolute adsorption is:

$$n_a = n_{max}\exp\left[-\left[\frac{RT}{\varepsilon}\right]^m \ln^m\left(\frac{P_0}{P}\right)\right] \qquad (3)$$

where n_{max}, ε, and P_0 must be determined for the pressure and temperature range of interest. The exponent m was preferentially set to 2, which is a special case of the D-A model corresponding to the Dubinin-Radushkevich equation. Czerny *et al.* showed that fitting the characteristic free energy of adsorption, ε, tends to vary linearly with temperature [12]. Thus, the characteristic free energy of adsorption is given by:

$$\varepsilon = \alpha + \beta T \qquad (4)$$

where α and -β are the enthalpic factor and the entropic factor, respectively.

Combining equations 1-4, experimental excess adsorption isotherms are fitted using the following equation:

$$n_{ex} = n_{max}\exp\left[-\left[\frac{RT}{\alpha+\beta T}\right]^2 \ln^2\left(\frac{P_0}{P}\right)\right] - \rho_g V_a \qquad (5)$$

where n_{max}, α, β, P_0, and V_a are the fitting parameters. The hydrogen adsorption data used in the present analysis primarily came from sources within the HSECoE [10, 11, 14, 17, 18, 19, 20, 21, 22, 23]. These internal isotherm data sets were also augmented with several external sources [3, 13, 24].

The isosteric heat of adsorption ($-\Delta\overline{h_a^0}$), which is also based on the adsorption isotherm data, can be calculated by the following equation provided by Myers and Monson [25]:

$$\Delta\overline{h_a^0} = -RT^2\left[\frac{\partial \ln P}{\partial T}\right]_{n_a,V} = -\alpha\sqrt{-\ln\left(\frac{n_a}{n_{max}}\right)} \qquad (6)$$

This non-constant heat of adsorption is used within the energy balance to equation to account for the changes in temperature within hydrogen adsorption/desorption.

PARAMETRIC STUDY

After the adsorbent had been characterized using the equations from the preceding section, the remaining portions of the hydrogen storage system can be design. Table 1 provides the major cryo-adsorbent hydrogen storage system design components and the number of variations initially considered each within the parametric analysis. Note that the total combination of all parametric study options totals over 17 billion, which is far too many to list in this article (but are available upon request).

Table 1. Parametric study components – Initial list

Component Categories	Variations
Adsorbent materials – including augmented material conditions/combinations	20
Media packing densities	5
Internal heat exchanger – all design options	48
Pressure vessel types	6
Pressure vessel L-to-D ratios	6
Pressure vessel endcap options	3
Insulation options	6
Full tank pressures	32
Full tank temperatures	22
Empty tank temperatures (related to full tank temperatures)	8

Powder activated carbon (AX-21 and MaxSorb) and the metal organic framework MOF-5™ were examined for this work. MOF-5™ was mechanically compacted into pucks of varying densities [17, 18, 20] both with and without thermal enhancement using expanded natural graphite (ENG). Additional adsorbent material variations included combining more than one adsorbent material, such as filling in the gaps between compacted pucks with powder adsorbent. In addition, several packing densities were used due to either shape limitation or to reduce estimate manufacturing costs. Table 2 provides D-A parameters used for the several adsorbent options.

Table 2. D-A parameters for select adsorbents

Parameter		Activated Carbon	Powder MOF-5™	0.32 g/cc MOF-5™	0.52 g/cc MOF-5™
ρ_{ads}	[kg/m^3]	270.0	130.0	322.0	520.0
α	[J/mol]	3080.0	2895.13	2095.25	2734.14
β	[J/mol/K]	18.90	15.2912	22.632	15.70
n_{max}	[mol/kg]	71.60	96.4317	154.815	69.378
P_0	[Pa]	1.470e9	1.387e9	3.156e9	9.205e8
V_a	[m^3/kg]	0.00143	0.00170	0.00220	0.00114
V_v	[m^3/kg]	0.00290	0.00725	0.00261	0.00143

Including all design options for specific internal heat exchanges, 4 dozen possible internal heat exchangers were considered. These heat exchangers include everything from a simple centerline resistance heater (such as those found in CcH2 applications) to a complex micro-channel heat exchangers. More will be said on these heat exchanger designs below when describing the system diagrams.

Once the internal heat exchanger and adsorbent were selected, the pressure vessel was designed around them. The design script used to create the pressure vessel was based on the *H₂ Tank Mass and Cost Estimator*, which was nicknamed the "Tankinator". This Excel design tool was written by partners within the HSECoE at PNNL and Hexagon-Lincoln and can be downloaded from http://www.hsecoe.org/models.php. Just like the original, the adapted script used in the current work relies on hoop stress and von Mises stress calculations at the design temperature and pressure to create a several different pressure vessel types for cross-comparison. These hypothetical pressure vessel designs are not all inclusive, but provide a useful scoping tool to compare estimate gravimetric, volumetric, and cost performance during the conceptual phase of design.

The balance of plant (BOP) is the last step in creating the on-board vehicle hydrogen storage system. While these components are relatively similar, there are several keys differences based on the design of the internal heat exchanger. Table 3 provides a list of typical BOP components. More will be said about the specific BOP designs below when describing the system diagrams.

Table 3. List of typical BOP components

Insulated H₂ wetted tubing	Micron in-line filter
H₂ wetted tubing	Pressure relief device
3-way Solenoid valve	Multi-port receptacle
Separation/Isolation Valve/Connector	External heat exchanger/ radiator
Check valve	Fuel cell coolant
Pressure regulator	Coolant tubing
Pressure gauge	Hose clamps
Temperature sensor	H₂ fittings
Pressure vessel burst disk	Pressure vessel vacuum port

Prior to performing the parametric study of possible on-vehicle cryo-adsorbent hydrogen storage system designs, the individual components and component combinations were examined to eliminate unrealizable systems. For example, the flow-through cooling (FTC) internal heat exchanger design did not work well with compacted adsorbents and, thus, these combinations were removed. Additionally, several internal heat exchanger designs could not handle the heat transfer requirement and were also eliminated.

Several engineering constraints were also implemented, which further reduced the total number of possible system designs. For example, while the refueling station forecourt is beyond the scope of the present work, the cooling capabilities of the forecourt is assumed to be limited to LN₂ temperatures, which also limits the minimum full tank temperature to 80 K. Additionally, Type 4 carbon fiber vessels with plastic liners were not considered due to the liner separation issues at cryogenic temperatures and low pressures (at time of the analysis). In addition, the aluminum version of the Type 1 pressure vessel options was the only one considered due to its decreased mass and cost compared to the other options.

Table 4. Parametric study components – Reduced list

Component Categories	Variations
Adsorbent materials – including augmented material conditions/combinations	12
Media packing densities	5
Internal heat exchanger – all design options	30
Pressure vessel types	2
Pressure vessel L-to-D ratios	3
Pressure vessel endcap options	3
Insulation options	1
Full tank pressures	12
Full tank temperatures	5
Empty tank temperatures (related to full tank temperatures)	8

After making the above and additional reductions to the parametric study components list, the total number of system design options has dropped below 16 million combinations, a full three orders of magnitude reduction. The updated reduced parametric study components list is shown in Table 4.

While there are several ways to evaluate the results of the parametric analysis, the three most important results were the estimate system cost, volumetric capacity ($H_{2,usable}$ mass / total system volume), and gravimetric capacity ($H_{2,usable}$ mass/ total system mass), in that order. The analysis results were then ranked based on maximum estimate gravimetric and volumetric capacities coupled with minimum estimate total system cost. Based on these rankings, the final two cryo-adsorbent hydrogen storage system designs were chosen, called the *HexCell* and *MATI* system designs based on the internal heat exchangers used. Both system met the DOE goal for storing 5.6 kg of $H_{2,usable}$.

Figure 1 shows the system diagram for the *HexCell* system design, with system information provided in Table 5. This system is characterized by the internal heat exchanger, nicknamed the *HexCell*, which consists of longitudinal
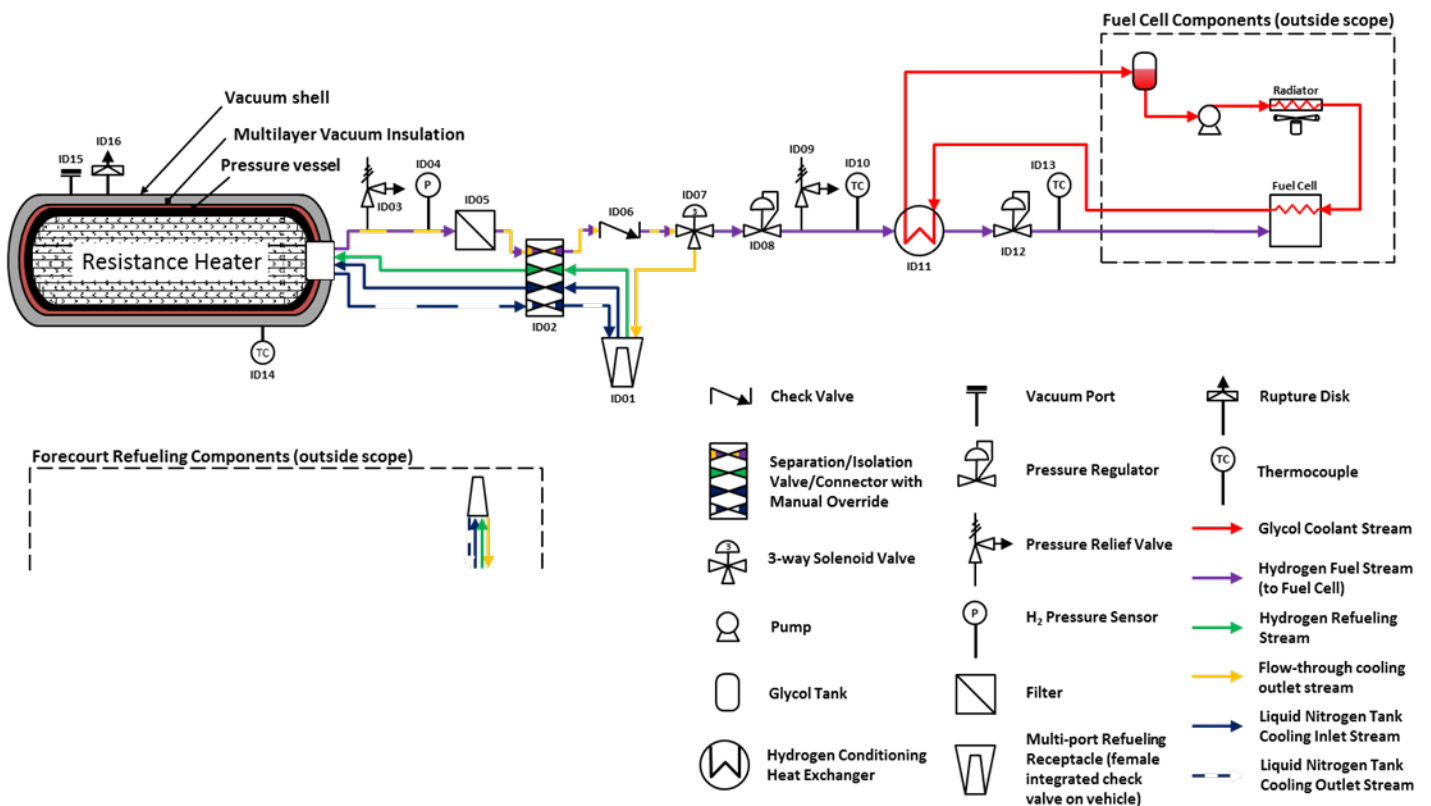

Figure 1. *HexCell* system diagram: Type 1 aluminum pressure vessel with powder MOF-5^{TM} in a hexagonal channel flow-through cooling heat exchanger with rod resistance heaters.

hexagonal channels that are lanced for cross-sectional H_2 flow. The *HexCell* relies on flow-through cooling (FTC), which flows LN_2-temperature H_2 through the MOF-5™ powder within the pressure vessel to simultaneously cool the MOF-5™ and provide H_2 for adsorption. Warm H_2 that is not adsorbed is flowed out of the pressure vessel back to the refueling forecourt to be recaptured and cooled for future use. The hexagonal channels are lanced to allow the gas to pass freely between the hexagonal channels. The *HexCell* also has rod resistance heaters spaced throughout the hexagonal channels to heat the adsorbent during vehicle operation to desorb H_2 and maintain the internal tank pressure necessary for fuel cell operation.

The pressure vessel for the *HexCell* system design is an aluminum Type 1 pressure vessel designed with a safety factor of 2.5 and a 2:1 L-to-D ratio. The Type 1 pressure vessel was chosen over the Type 3 pressure vessel because the pressure vessel cost is significantly lower with no increased volume for design pressures below 100 bar. While more difficult to install on-board a vehicle, an L-to-D ratio of 2:1 was used to maximize the volumetric capacity and gravimetric capacities. The pressure vessel is wrapped with 1" MLVI and a 2-mm aluminum outer shell for dormancy and impact purposes. Note that while many vehicles use multiple smaller tanks for easier installation within existing vehicle frameworks, only single-tank system were considered in the present work to minimize the mass, volume, and cost of the system designs.

Downstream of the pressure vessel are several BOP components to ensure the desired vehicle operation. For example, a H_2 conditioning heat exchanger is installed downstream of the pressure vessel to heat the H_2 delivered to the FC for above the required minimum -40 ºC using waist heat from the FC. In addition, the FC rail pressure (minimum pressure needed for operation) of 5 bar is maintained using two separate pressure regulators, one on either side of the H_2 conditioning heat exchanger.

The system diagram and key system information for the *MATI* system design are shown in Figure 2 and Table 5, respectively. *MATI* stands for Modular Adsorbent Tank Insert, which is a microchannel isolated-fluid system designed by OSU for the HSECoE [26]. A schematic of the *MATI* internal heat exchanger within a generalized pressure vessel is shown in Figure 3. During refueling, LN_2 flow through the microchannel plates isolated from the internals of the pressure vessel to cool the compacted MOF-5™ pucks via conduction while H_2 flows into the pressure vessel to be adsorbed. This continues of the target full tank operating pressure and temperature are reached. Alternately, during
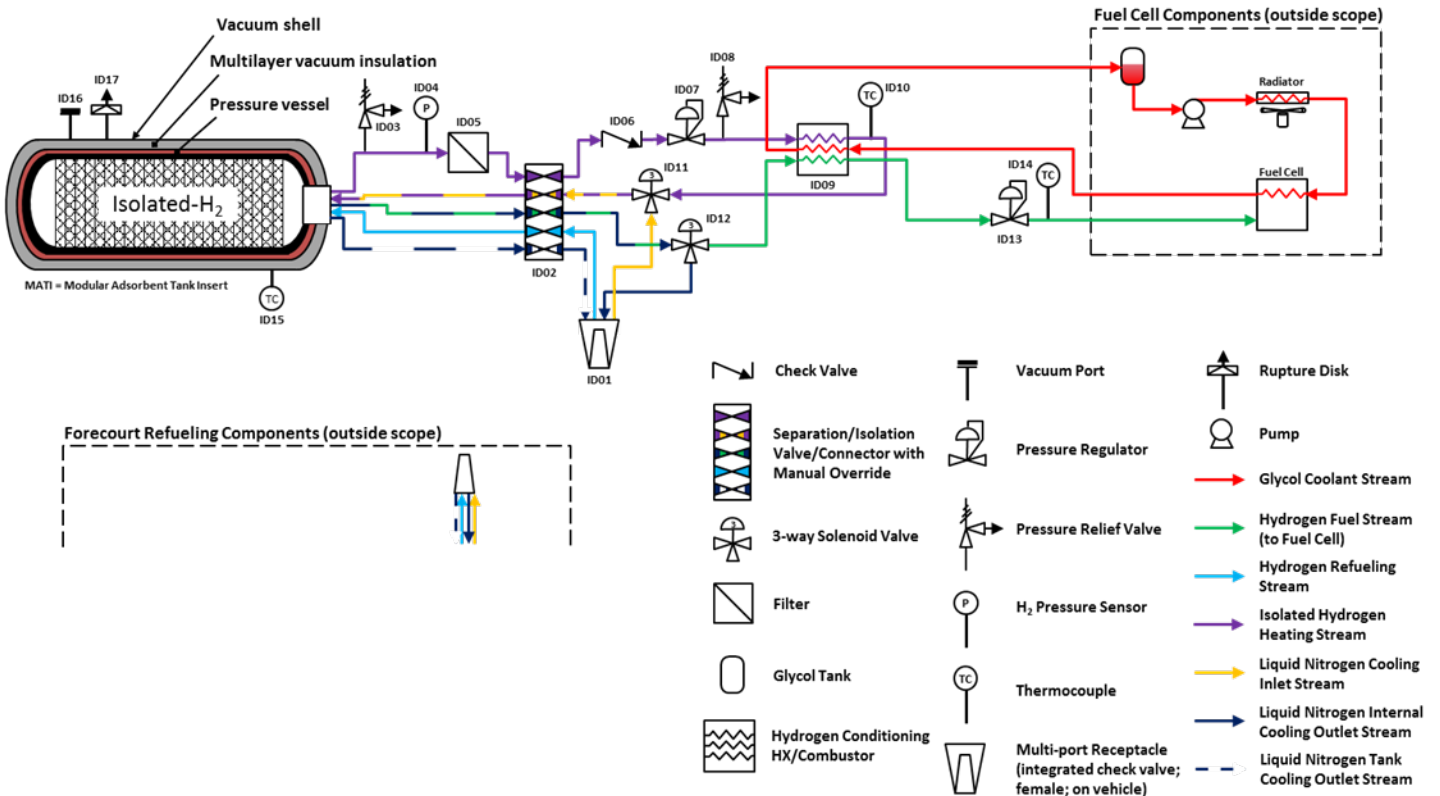

Figure 2. *MATI* system diagram: Type 1 aluminum pressure vessel with compacted MOF-5^{TM} pucks in a microchannel isolated-fluid heat exchanger system.

vehicle operation, H_2 flows from the pressure vessel downstream to the H_2-conditioning heat exchanger (first pass), where H_2 flows back to the pressure vessel and into the *MATI* through the headers. For the *MATI* system design, the H_2-conditioning heat exchanger must also contain a microchannel H_2-combustor that uses up to 0.5% of the H_2 flow to increase the temperature above what is possible from the FC radiator. This ensures that the MOF-5™ can maintain the needed H_2 desorption rates to maintain the needed internal tank pressure. Once the heated-H_2 passes through the inside of the *MATI*, the H_2 is cooled below the FC's minimum required temperature and then flows back through the H_2-conditioning heat exchanger (second pass) where it is heated above -40 ºC for use by the FC.

Table 5. System design specifications

	HexCell	MATI
Tank operating pressure [bar]	5 – 100	5 – 100
Tank operating temperature [K]	80 – 140	80 – 140
$H_{2,usable}$ [kg]	5.6	5.6
Internal tank volume [L]	188.4	180.1
Tank L-to-D ratio	2:1	2:1
Aluminum PV thickness [mm]	14.00	13.06
MLVI thickness [mm]	25.4	25.4
Outer Al shell thickness [mm]	2.0	2.0
Total system mass [kg]	140.99	141.59
Total system volume [L]	287.70	246.03
Total system cost*	$2219	$2616
System Gravimetric Capacity [$g_{H2,usable}/g_{system}$]	0.03974	0.03957
System Volumetric Capacity [$g_{H2,usable}/L_{system}$]	19.47	22.77

*System costs are for system-to-system comparison purposes only and not intended to represent the actual market cost of these systems.

The pressure vessel for the *MATI* system design is also a single aluminum Type 1 pressure vessel designed with a safety factor of 2.5 and a 2:1 L-to-D ratio. As with the *HexCell* system, the pressure vessel is also wrapped with 1" MLVI and a 2-mm aluminum outer shell for dormancy and impact 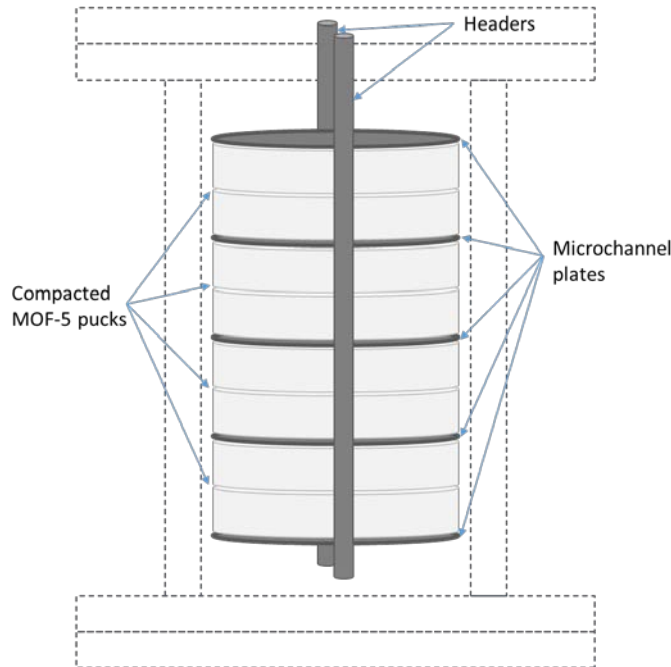purposes. Downstream of the pressure vessel, the BOP has several additional/different components compared to the *HexCell* system design. Specifically, the downstream H_2-conditioning heat exchanger is designed for multiple passes and contains a micro-combustor, as described in the previous paragraph. In addition, there are additional components and H_2 tubing to support the multiple passes between the pressure vessel and the H_2-conditioning heat exchanger.

ADDITIONAL TRENDS & OBSERVATIONS

While the *HexCell* and *MATI* system designs both ranked highly within the constraints of the current parametric study, neither system design meets the DOE's gravimetric capacity or volumetric capacity targets [1]. By analyzing the designs more closely, trends can be seen that could produce future system designs that do meet or surpass the targets. Figure 4 shows percentage breakdowns of the total system mass, volume, and cost for both the *HexCell* and *MATI* system designs. Note that the total system mass, volume, and cost are listed in Table 5.

For both system designs, the adsorbent material accounts for more than half of the system
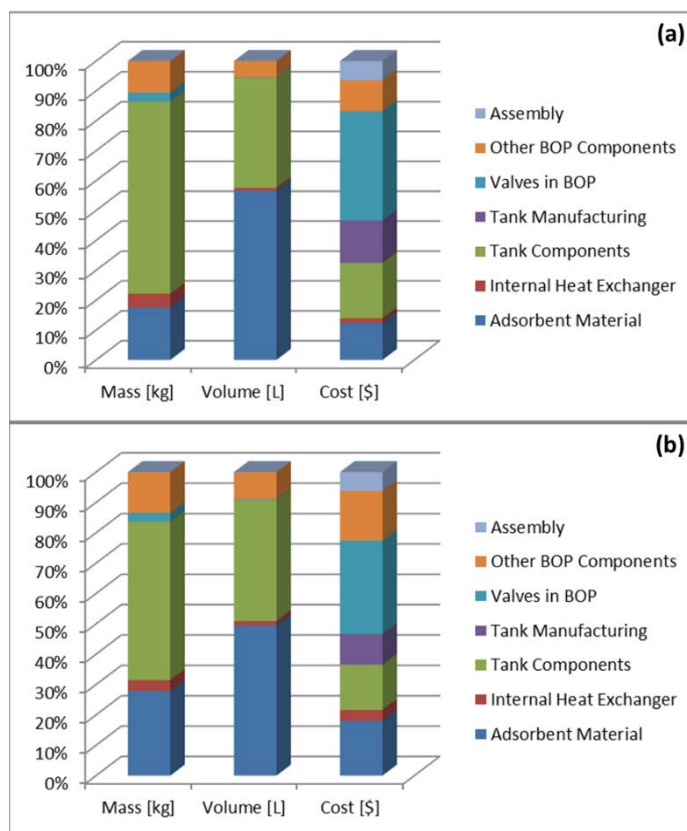

Figure 3. Schematic of a generic *MATI* internal heat exchanger within a pressure vessel.

Figure 4. Total system mass, volume, and cost breakdowns for the a) *HexCell* and b) *MATI* system designs.

volume. If MOF-5™ were replaced by an adsorbent with a higher H_2 storage capacity, this volume and the volume of the overall system could be greatly reduced. This is part of the argument behind adsorbent densification. Note that the adsorbent H_2 storage capacity is defined as the difference in H_2 storage between the full tank temperature and pressure and the empty tank temperature and pressure. Thus, an adsorbent may store more total H_2 than MOF-5™ at the same temperature and pressure but not have a higher capacity because it is based on the difference and not an absolute value. The tank components (pressure vessel, insulation, etc.) make up most the total system mass for both system designs because both systems use Type 1 aluminum tanks. If a Type 3 tank were used at the systems' 100 bar maximum operating pressure instead, then the total system mass would be greatly reduced while maintaining a similar system volume. However, Type 1 pressure vessels are less expensive than the comparable Type 3 pressure vessels and were chosen to keep the overall system costs as low as possible.

The system cost distribution within Figure 4 appears relatively well distributed between the individual system components. Upon closer evaluation, the valves within the BOP account for the highest single impact to the system cost. Specifically, the 3-way solenoid valve and the pressure regulator valves make up approximately 1/3 of the estimate total system cost. Thus, a lower cost alternative that is still rated for cryogenic hydrogen at the operating pressures would have the highest benefit.

While an adsorbent with a higher H_2 storage capacity may not have been developed yet, mechanical compaction may provide an engineering solution to increase an existing adsorbent's volumetric capacity. Figure 5 shows the capacity changes for various compaction levels for a MOF-5™ H_2 storage system utilizing a *MATI* internal heat exchanger in a Type 1 aluminum pressure vessel with a 100-bar full tank pressure. Note that the 0.0 g/cc compaction density is a CcH_2 with the same operating conditions. As expected, the volumetric capacity increases with increasing compaction level for all operating conditions shown, but this comes at the cost of the decreased gravimetric capacity with increasing compaction level. However, the volumetric capacity increase is not linear toward the highest MOF-5™ compaction densities for the 70 K, 80 K, and 90 K data sets. The compressed gas portion of the H_2 storage remains relatively constant within a given temperature data set at the 100-bar operating pressure, which means the decreased H_2 storage can be attributed to the adsorbed H_2 portion. Because mechanical compaction is used, it is hypothesized that the adsorption sites may be damaged at higher levels of compaction. This also implies that there is an optimal level of compaction, but this will need to be confirmed experimentally (which is beyond the scope of the present work).

Figure 6 shows gravimetric capacity and volumetric capacity results for powder MOF-5™ in the *HexCell* system design and two levels of compacted MOF-5™ (0.32 g/cc and 0.52 g/cc) in the *MATI* system design at various operating conditions. Each of these systems utilized an aluminum Type 1 pressure vessel with a 2:1 L-to-D ratio at various operating pressure with a 60 K temperature swing between the full and empty tank temperatures. As is expected, the volumetric capacity increases with decreased operating temperatures and increased full tank pressure. The volumetric capacity seems to approach a plateau for pressures above 100 bar across all of the operating temperatures shown. This trend can be attributed to the decreased excess H_2 stored compare to pure CcH2 at higher pressures coupled with the increases pressure vessel wall thickness needed at the higher pressures. In addition, across all systems shown in Figure 6, the gravimetric capacity has a definitive maximum for each set of operating temperatures, which can also be attributed to the decreased excess H_2 stored coupled with the thicker pressure vessel wall.
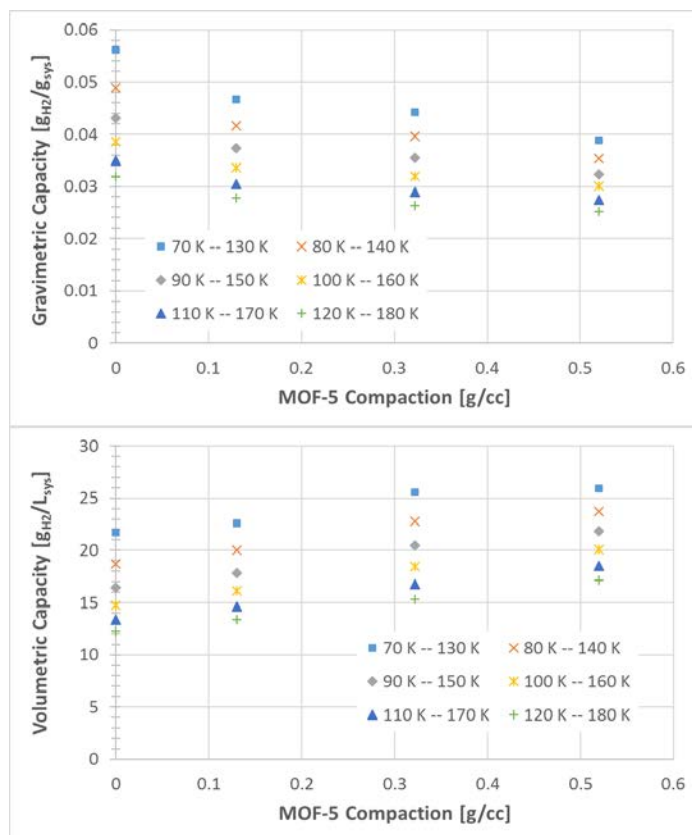
Figure 5. MOF-5 compaction in a *MATI* system design with an aluminum Type 1 pressure vessel and a 100-bar full tank pressure.

Figures 4-6 could be made for another adsorbent material, a different pressure vessel (such as a Type 3 tank), or any number of parametric study options, but will not be described here for the sake of brevity. Note that the trends described in the present paper hold throughout the parametric analysis performed.

CONCLUSIONS

Cryo-adsorbent based hydrogen storage systems for fuel cell vehicles were evaluated using numerical models that were validated against experimental data. These models simultaneously solve equations for adsorbent thermodynamics together with the heat, mass, and momentum conservation equations. These models also utilize the real gas thermodynamic properties for hydrogen. Model predictions were compared to data for charging and discharging both activated carbon and MOF-5™ systems in various conditions (powder, compacted, etc.). The full system models were used in a parametric analysis to compare prospective system design performance given specific options, such as the adsorbent materials and their condition, pressure vessel types, internal heat exchangers, and operating conditions.

Given various physical restrictions and engineering restrictions, the system design options is reduced from billions down to millions of option. These design options are then ranked based on their estimate system cost, volumetric capacity, and gravimetric capacity. Using these rankings, the two system designs were chosen, the *HexCell* and *MATI* system designs. Additionally, trends and comparisons from the parametric analysis provide guidance for areas of improvement and future research directions.

Note that prior to performing the above parametric analysis for the HSECoE, several adsorbent materials were eliminated from consideration due to a lack of available experimental data. Using the tools described in this work, these materials could now be evaluated if the necessary data was now available.

ACKNOWLEDGMENTS

REFERENCES

[1] https://energy.gov/eere/fuelcells/doe-technical-targets-onboard-hydrogen-storage-light-duty-vehicles
[2] Satyapal, S., Petrovic, J., Read, C., Thomas, G., and Ordaz, G., (2007), "The U.S. Department of Energy's National Hydrogen Storage Project: Progress towards meeting hydrogen-powered vehicle requirements." *Catalysis Today* **120**, 246-256.
[3] Ahluwalia, R.K., Hua, T.Q., Peng, J.-K., Lasher, S., McKenney, K., Sinha, J., and Gardiner, M., (2010), "Technical assessment of cryo-compressed hydrogen storage tank systems for automotive applications." *Int. J. Hydrogen Energy* **35**, 4171-4184.
[4] Hardy, B.J. and Anton, D.L., (2009), "Hierarchical methodology for modeling hydrogen storage systems. Part I: Scoping models." *Int. J. Hydrogen Energy* **34**, 2269-2277.
[5] Hardy, B.J. and Anton, D.L., (2009), "Hierarchical methodology for modeling hydrogen storage systems. Part II: Detailed models." *Int. J. Hydrogen Energy* **34**, 2992-3004.
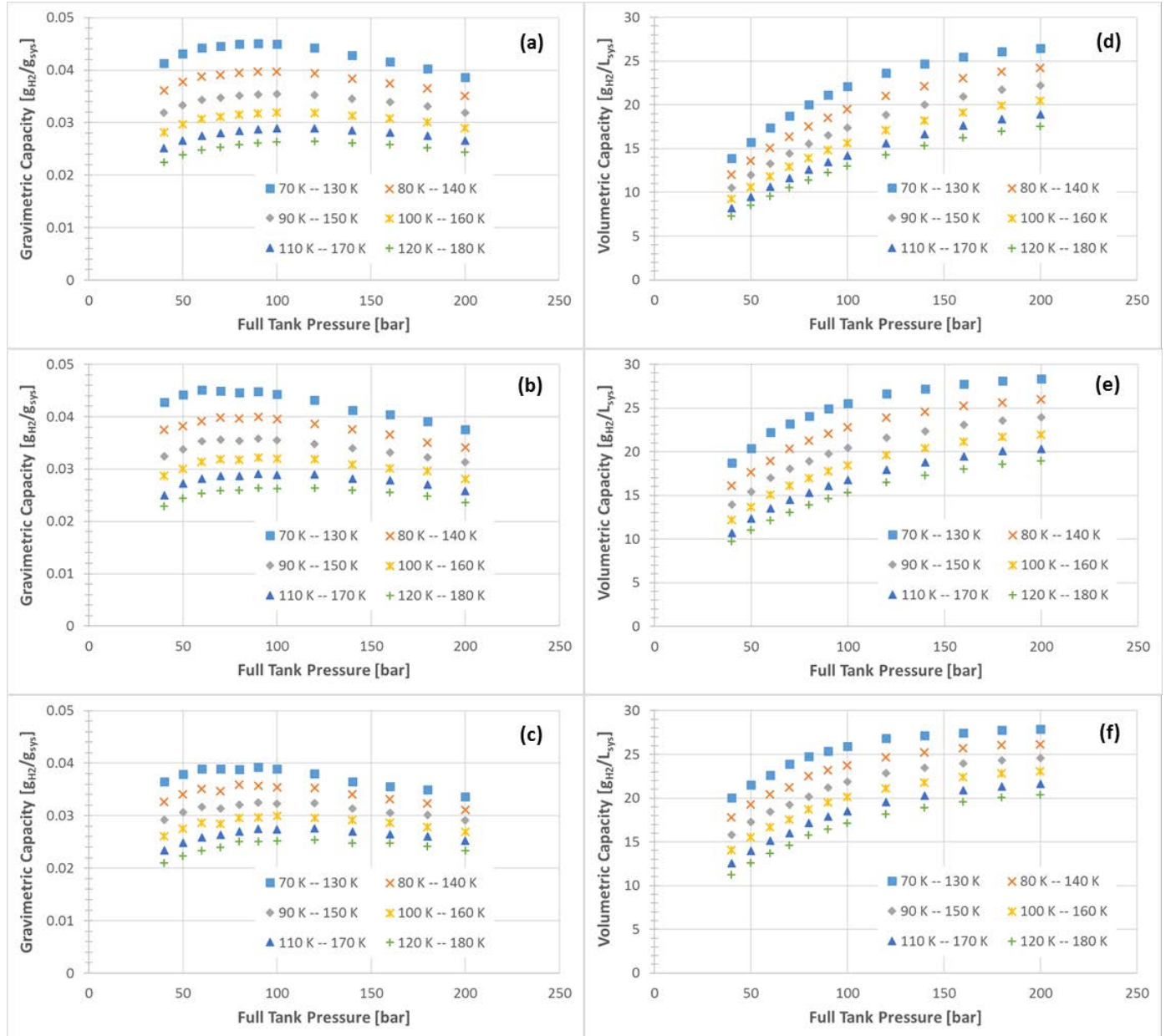
Figure 6. (a, b, c) Gravimetric capacity and (d, e, f) volumetric capacity trends for (a, d) powder MOF-5™ *HexCell*, (b, e) 0.32 g/cc compacted MOF-5™ *MATI*, and (c, f) 0.52 g/cc compacted MOF-5™ *MATI* system designs, with 2:1 L-to-D ratio aluminum Type 1 pressure vessels.

[6] Garrison, S.L., Hardy, B.J., Gorbounov, M.B., Tamburello, D.A., Corgnale, C., van Hassel, B.A., Mosher, D.A., and Anton, D.L., (2012), "Optimization of internal heat exchangers for hydrogen storage tanks utilizing metal hydrides." *Int. J. Hydrogen Energy* **37**, 2850-2861.

[7] Mohan, G., Prakash Maiya, M., and Srinivasa Murthy, S., (2007), "Performance simulation of metal hydride hydrogen storage device with embedded filters and heat exchanger tubes." *Int. J. Hydrogen Energy* **32**, 4978-4987.

[8] Botzung, M., Chaudourne, S., Gillia, O., Perret, C., Latroche, M., Percheron-Guegan, A., and Marty, P., (2008), "Simulation and experimental validation of a hydrogen storage tank with metal hydride." *Int. J. Hydrogen Energy* **33**, 98-104.

[9] Raju, M., Ortmann, J.P., and Kumar, S., (2010), "System simulation model for high-pressure metal hydride hydrogen storage systems." *Int. J. Hydrogen Energy* **35**, 8742-8754.

[10] Richard, M.-A., Benard, P., and Chahine, R., (2009), "Gas adsorption process in activated carbon over a wide temperature range above the critical point. Part 1: modified Dubinin-Astakhov model." *Adsorption* **15**, 43-51.

[11] Richard, M.-A., Benard, P., and Chahine, R., (2009), "Gas adsorption process in activated carbon over a wide temperature range above the critical point. Part 2: conservation of mass and energy", *Adsorption* **15**, 53-63.

[12] Czerny, A.M., Benard, P., and Chahine, R., (2005), "Adsorption of nitrogen on granular activated carbon: experiment and modeling." *Langmuir* **21**, 2871-2875.

[13] Zhou, W., Wu, H., Hartman, M.R., and Yildirim, T., (2007), "Hydrogen and methane adsorption in metal-organic frameworks: A high-pressure volumetric study." *J. Phys. Chem. C* **111**, 16131-16137.

[14] Hardy, B., Corgnale, C., Chahine, R., Richard, M.-A., Garrison, S., Tamburello, D., Cossement, D., and Anton, D., (2012), "Modeling of adsorbent based hydrogen storage systems." *Int. J. of Hydrogen Energy* **37**, 5691-5705.

[15] Pasini, J.-M., van Hassel, B.A., Mosher, D.A., and Veenstra, M.J., (2012), "System modeling methodology and analysis for materials-based hydrogen storage." *Int. J. Hydrogen Energy* **37**, 2874-2884.

[16] Thornton, M., Brooker, A., Cosgrove, J., Veenstra, M., and Pasini, J.M., (2012), "Development of a vehicle-level simulation model for evaluating the trade-off between various advanced on-board hydrogen storage technologies for fuel cell vehicles." *SAE Technical Paper* **2012-01-1227**.

[17] Xu, C., Yang, J., Veenstra, M., Sudik, A., Purewal, J.J., Ming, Y., Hardy, B.J., Warner, J., Maurer, U., and Siegel, D.J., (2013), "Hydrogen permeation and diffusion in densified MOF-5 pellets." *Int. J. Hydrogen Energy* **38** (8), 3268-3274.

[18] Purewal, J.J., Liu, D., Yang, J., Sudik, A., Siegel, D.J., Maurer, S., and Muller, U., (2012), "Increased volumetric hydrogen uptake of MOF-5 by powder densification." *Int. J. Hydrogen Energy* **37**, 2723-2727.

[19] Richard, M.-A., Cossement, D., Chandonia, P.-A., Chahine, R., Mori, D., and Hirose, K., (2009), "Preliminary evaluation of the performance of an adsorption-based hydrogen storage system." *AIChE Journal* **55** (11), 2985-2996.

[20] Liu, D., Purewal, J.J., Yang, J., Sudik, A., Maurer, S., Mueller, U., Ni, J., and Siegel, D.J., (2012), "MOF-5 composites exhibiting improved thermal conductivity." *Int. J. Hydrogen Energy* **37**, 6109-6117.

[21] Juan-Juan, J., Marco-Lozar, J.P., Suarez-Garcia, F., Cazorla-Amoros, D., and Linares-Solano, A., (2010), "A comparison of hydrogen storage in activated carbons and a metal-organic framework (MOF-5)." *Carbon* **48**, 2906-2909.

[22] Marco-Lozar, J.P., Juan-Juan, J., Suarez-Garcia, F., Cazorla-Amoros, D., and Linares-Solano, A., (2012), "MOF-5 and activated carbons as adsorbents for gas storage." *Int. J. Hydrogen Energy* **37** (3), 2370-2381.

[23] Yang, J., Sudik, A., Wolverton, C., and Siegel, D.J., (2010), "High capacity hydrogen storage materials: attributes for automotive applications and techniques for materials discovery." *Chem. Soc. Rev.* **39**, 656-675.

[24] Ahluwalia, R.K. and Peng, J.K., (2009), "Automotive hydrogen storage system using cryo-adsorption on activated carbon." *Int. J. Hydrogen Energy* **34**, 5476-5487.

[25] Myers, A.L. and Monson, P.A., (2002), "Adsorption in porous materials at high pressure: Theory and experiment." *Langmuir* **18**, 10261-10273.

[26] Steigleder, L.J., (2012), "A microchannel-based thermal management system for hydrogen storage adsorbent beds." *M.S. Thesis,* **Oregon State University**.

ANNEX A

DOE EERE ONBOARD HYDROGEN STORAGE TECHNICAL TARGETS [28]

Technical System Targets: Onboard Hydrogen Storage for Light-Duty Fuel Cell Vehicles [a] (updated May 2015)			
Storage Parameter	**Units**	**2020**	**Ultimate**
System Gravimetric Capacity: Usable, specific-energy from H_2 (net useful energy/max system mass)[b]	kWh/kg (kg H_2/kg system)	1.8 (0.055)	2.5 (0.075)
System Volumetric Capacity: Usable energy density from H_2 (net useful energy/max system volume)[b]	kWh/L (kg H_2/L system)	1.3 (0.040)	2.3 (0.070)
Storage System Cost : • Fuel cost [c]	$/kWh net ($/kg H_2) $/gge at pump	10 333 2-4	8 266 2-4
Durability/Operability: • Operating ambient temperature [d] • Min/max delivery temperature • Operational cycle life (1/4 tank to full) • Min delivery pressure from storage system • Max delivery pressure from storage system • Onboard Efficiency [e] • "Well" to Powerplant Efficiency [e]	ºC ºC Cycles bar (abs) bar (abs) % %	-40/60 (sun) -40/85 1500 5 12 90 60	-40/60 (sun) -40/85 1500 5 12 90 60
Charging / Discharging Rates: • System fill time (5 kg) • Minimum full flow rate • Start time to full flow (20°C) • Start time to full flow (-20°C) • Transient response at operating temperature 10%–90% and 90%–0%	min (kg H_2/min) (g/s)/kW s s s	3.3 (1.5) 0.02 5 15 0.75	2.5 (2.0) 0.02 5 15 0.75
Fuel Quality (H_2 from storage) [f]:	% H_2	SAE J2719 and ISO/PDTS 14687-2 (99.97% dry basis)	
Environmental Health & Safety: • Permeation & leakage [g] • Toxicity • Safety	- - -	Meets or exceeds applicable standards	
Loss of useable H_2 [h]	(g/h)/kg H_2 stored	0.05	0.05

* Useful constants: 0.2778 kWh/MJ; Lower heating value for H_2 is 33.3 kWh/kg H_2; 1 kg H_2 ≈ 1 gal gasoline equivalent (gge)

Footnotes to Target Table:

[a] Targets are based on the lower heating value of hydrogen, 33.3 kWh/kg H_2. Targets are for a complete system, including tank, material, valves, regulators, piping, mounting brackets, insulation, added cooling capacity, and all other balance-of-plant components. All capacities are defined as useable capacities that could be delivered to the fuel cell power plant. All targets must be met at the end of service life (approximately 1500 cycles or 5000 operation hours, equivalent of 150,000 miles).

[b] Capacities are defined as the useable quantity of hydrogen deliverable to the powerplant divided by the total mass/volume of the complete storage system, including all stored hydrogen, media, reactants (e.g., water for hydrolysis-based systems), and system components. Capacities must be met at end of service life. Tank designs that are conformable and have the ability to be efficiently package onboard vehicles may be beneficial even if they do not meet the full volumetric capacity targets.